Research paper

# Helicopter modelling and study of the accelerated rotor

S. Castillo-Rivera*, M. Tomas-Rodriguez

*School of Mathematics, Computer Science & Engineering, City University of London, London, United Kingdom*

ARTICLE INFO

*Article history:*
Received 4 June 2017
Revised 31 July 2017
Accepted 28 August 2017
Available online 5 September 2017

*Keywords:*
Helicopter
Rotor
Acceleration
Hinge
Vibration

ABSTRACT

This work presents a helicopter dynamic model that captures the fuselage vibrations for an accelerated main rotor. Some rotor parameters are modified with the purpose of study their impact on the rotorcraft. Being this, a tool that allows to predict vibrations on the helicopter. The rotorcraft model has been built up by using VehicleSim, software specialized in modelling mechanical systems composed by rigid bodies. The rotors are articulated, the main rotor takes into account flap, lag and feather degrees of freedom for each of the equispaced blades and their dynamic couplings. The dynamic performance and the control action are embedded in a single code, thereby VehicleSim does not require external connection to other software package. This generates some advantages such as to reduce the compilation time. The control methodology makes use of PID controllers (Proportional, Integral, Derivative), which allows to use VehicleSim commands exclusively. The state space matrices have been obtained in order to analysis the uncoupled main rotor flap and lag modes. The detection of vibrations from the offset flap hinge as well as the lag hinge are not straightforward tasks and this helicopter model provides an accurate tool to study these. A short time Fourier transform processing is used to analysis the vibrations and these have shown to agree with the expected behaviour.



## 1. Introduction

Helicopters are adaptable for their different applications and these have been increased over the years. They have roles such as monitoring of traffic, air ambulance, fire fighting, etc. [1]. These trade demand the vibrations reduction to accomplish a better reliability of structures, efficiency and greater comfort [2]. It is well known that the rotorcrafts are prone to higher vibration levels than the aircrafts. In fact, the vibration level in helicopter is of the order of five times the vibration levels located in fixed wing aircraft [3]. It is found that these vibrations are due to the rotorcraft configuration as well as their varying velocities.

Faithful reproduction of the helicopter dynamical vibration requires a tough modelling process and the used of simulation techniques, which can be carried out by using the different software packages existent, see [4,5]. In fact, the interaction between the main rotor and the fuselage needs a particular attention. In order to reduce the cost of the experimental tests and to obtain more accurate outcomes, these type of simulations should be considered.

Practical examples can be found wherein the measure and the analysis of helicopter vibrations have been studied to identify defects on their operating components. Stupar et al. [6] presented and implemented a vibration testing methodology to figure out the correct performance of the rotating components. The tests were done on a military Gazelle helicopter SA-342. The practical methodology was carried out in the following steps: (a) To determine the rotating systems and subsystems the operating frequencies. (b) To select a number of locations on the structure for measuring the vibrations on the ground. (c) To choose an inner location at the structure, being this a specific point for the corresponding flight tests. This allowed to determine the helicopter features and the demands for any testing actions. The test was conducted with an equipment configuration such as 12 channels NetdB12 - 01 Metravib digital analyser and data collector, in order to measure the vibrations in real time. 5 accelerometers B&K type 4393 and 1 tachometer. Several accelerometers were set up for recording the configuration on different positions and helicopter directions. As a result, a technical review of their relevant components and a disclosure of the failures on its surface were done. Furthermore, this method of measurement and analysis could be accomplished on different kind of aircraft for extending their operational life expectancy. The damage detection methods have been used by dos Santos et al. [7] to put forward experimental outcomes related to a helicopter main rotor blade. The methods used were the modal strain energy, and the coordinate modal assurance criterion (COMAC). Modal parameters were derived using experimental modal analysis and damage was inserted on the blade by linking a small mass to it, thereby, their properties were altered. The helicopter

* Corresponding author.
*E-mail address:* Salvador.Castillo-Rivera.1@city.ac.uk (S. Castillo-Rivera).

blade features were displayed and an experimental modal analysis was done. The damage was simulated to establish the blade vibration modes, under the impact of an unbalance of mass. A comparison was carried out between the studied cases. As a consequence of this, the COMAC damage indicator was less sensitive than the strain energy technique, due to the damage index was not able to find out the exact location of the added mass. The modal strain energy formulation handles a lot of approximations to work out the final damage index, on the contrary, this supplied the adequate detection possibilities and sensitivity.

The estimation of the unbalance force and the unbalance itself of a rigid rotor system during acceleration is a cumbersome task that it must be dealt with. Vibration generated by mass unbalance is a relevant factor, which restricting the performance of the rotating system. Zhou and Shi [8] presented a new method of the unbalance estimation for the rigid rotor during acceleration. The estimated unbalance was figured out, as a consequence of this, unbalance forces and moments were obtained as the states of the augmented system. This method could be applied to active balancing schemes for a rigid rotor or the active vibration control. The features of the transition vibration of a rotor when it passes its critical speeds throughout acceleration encourage an interest of disciplines such as the rotor design, active real-time balancing and active vibration control. In fact, the rotor study under constant acceleration has been tackled by Zhou and Shi [9]. This work provides an analytical unbalance response of the Jeffcott rotor. An analytical solution was derived for the unbalance response of the Jeffcott rotor during acceleration. The obtained solution showed that the motion was made up of three parts: (a) a transient vibration at damped natural frequency. (b) A synchronous vibration with the frequency of instantaneous frequency. (c) A suddenly occurring vibration at damped natural frequency. Zhou et al. [10] put forward an active balancing method to offset the unbalance of the rotor system during acceleration using an electromagnetic balancer. In order to reduce the impact on a rotor when it passed through its critical speeds, which is able to damage the system. An assessment was carried out to validate this method and the validation outcomes were shown. In this scheme, "instantaneous" influence coefficients at different speeds were calculated and stored in a look-up table. Afterward, a gain scheduling strategy was taken into account to remove the unbalance-induced vibration during acceleration established on the "instantaneous" influence coefficient table.

Furthermore, variable speed rotor studies are a research field for the rotorcraft operations improvement as well as the fuel consumption reduction. According to Misté and Benini [11], there are two main variable speed concepts, fixed-ratio transmission and continuously variable transmission rotors. The effect of these types of transmissions on the helicopter performance is calculated when both are working at their optimal speeds. This can be carried out using two different simulation tools, a turboshaft engine performance code and a helicopter trim simulation code for steady-state level flight. After a study done by the authors, fixed-ratio transmission was presented as a well process to diminish the fuel consumption at intermediate advancing speeds. However, continuously variable transmission advantages showed to be relevant in hover and in high speed forward flight.

The vibration impact and its determination upon the helicopter structural components in terms of frequency characteristics have been recently studied, Khaksar et al. [12] have developed in ABAQUS a 3D finite element method for a 349 Gazelle helicopter model. ABAQUS is a program based on the finite element method. It is able to resolve problems ranging from relatively simple linear analysis to the most complex nonlinear simulations [13]. The main advantage of this model is that, it can be used to predict the natural frequencies of the full structure. The model provides a tool to test the frequencies of the helicopter with different components. Often, it is overlooked the vibrations and the human body, Ceruti et al. [14] have reported about this matter. The authors describe the standard range of the vibrations on helicopters. However, a novelty aspect is shown i.e., the whole-body acceleration [15] displays medium-low frequencies in a range of 2–20 Hz.

In order to understand the limitations and shortcomings of controller designs to capture helicopter performance, the following considerations can be done. The flight control systems are able to classify as linear or nonlinear, these are established according to the controller requirements and the helicopter model that is built up. The linear control design is more applied and it has been run on the majority of helicopter platforms. It is more used due to the simplicity of the controller design, which reduces the computational complexity and the modelling time. However, nonlinear controllers are demanded for their theoretical contribution to the rotorcraft control problem [16]. In fact, Chen et al. [17] have recently developed the adaptive neural fault-tolerant control approach for the three degrees of freedom model helicopter in the presence of system uncertainties, unknown external disturbances and actuator faults. The unknown external disturbances as well as the unknown neural network approximation error were processed as a compound disturbance that was figured out with a nonlinear disturbance observer. The simulation results showed the effectiveness of the proposed adaptive control scheme. Cui et al. [18] have also developed an observer based backstepping control scheme for the attitude control problem of three degrees of freedom model helicopter with unknown external disturbance, unknown modelling uncertainties and unknown states. Backstepping control law was set up based on the estimated values of observers to obtain suitable tracking performance. The results displayed effectiveness of the designed control approach. Despite of these recent works have demonstrated to be efficient, they have been carried out for helicopters with three degrees of freedom. Both approaches must be extended to six degrees of freedom, in order to be extended to helicopters model more complex. On the other hand, the application of these control schemes would involve to use external software packages to VehicleSim. In here, a PID (Proportional, Integral, Derivative) methodology is applied in various subsystems of the helicopter model, as it is strong to accomplish the required objectives. The PID control methodology is implemented in VehicleSim, the main argument is that this allows to program an single code, being not necessary to use any additional software.

VehicleSim is a multibody software specialized in modelling mechanical systems composed by rigid bodies. It is used as main software package due to the helicopter nonlinear behaviour and equations of motions are provided. In addition to this, the state spaces matrices are also derived, being these an additional advantage with respect other software that can be found in the literature, see [5]. Furthermore, operational modal analysis of the rotating helicopter blade can find a support tool in this software. Due to it can facilitate the studies carried out in this field, as for example the work presented by Agneni et al. [19]. The authors estimated the damping ratios, natural frequencies and mode shapes without to measure the input forces. In this way, the system modal parameters were able to establish its operative conditions. The capability to improve the operational modal analysis procedure was also studied through whirl tower experimental tests. The proposed approach allowed the study of both the rotating frequency as well as the damping ratios as functions of the rotating speed. Although the estimate of the rotating frequencies was not sensitive to the different estimation approach, at least for the experimental data, noteworthy differences in the damping ratio estimates were described. An underestimate of the damping ratio of the modes with natural frequency close to the one the identified operational frequencies was identified.

Thus, this work studies the capability of VehicleSim to program an embedded code using VehicleSim commands exclusively. For this task and doing use of the VehicleSim features the blades are rigid and the flexibility is not tackled. Due to it is not mandatory to carry out in a first approach of VehicleSim as a modelling tool in such case. The rigid bodies and VehicleSim methodology are sufficient to achieve the objective fixed by the authors. At first sight, this would need to employ an external software, however the authors are currently studying its implementation in a single code, without requiring the performance of external commands to VehicleSim. In this way, the hugely complicate implementation process should be simplified.

This work simulates in a single code, the vibrations generated in an accelerated helicopter main rotor, when structural unbalance are also taken into account. The authors seek some advantages such as the portability and the reduction of the compilation time, being this an alternative tool to predict vibrations. In addition to this, it aims to shed light on the complex mechanisms that govern the rotor dynamics when an acceleration is presented. This is an improvement with respect to the works presented by Stupar et al. and co-workers [6,7]. Due to the vibration testing methodology to detect the correct performance of the rotating components, and the damage detection methods could find a simulation tool in this approach. Furthermore, the state space provided by VehicleSim can be a simulation alternative to the experimental modal analysis using by dos Santos et al. [7]. The studies carried out by Zhou and co-workers [8–10] could be extended to a helicopter main rotor model through of this implementation. Taking into account that variable speed rotor studies are a research field for the helicopter operations improvement. The helicopter model presented can be an alternative or complement to the two different simulation tools presented by Misté and Benini [11]. A multibody perspective is used to show an alternative procedure to face this cumbersome task. Thus, this contribution provides an alternative tool for rotorcraft vibrations prediction. Due to recent studies as the presented by Khaksar et al. [12], the vibration impact and its determination on the rotorcraft structural components have been dealt with by using finite element method.

In the view of these considerations, the main contributions of this paper can be summarized as: (a) To present a simulation approach for the accelerated main and tail rotors of a helicopter dynamic model, this task has been carried out using VehicleSim. It is a new approach implemented at an embedded code, which minimizes the complexity of the study of the helicopter dynamic performance as well as the action control. This derives advantages as the portability and the reduction of the compilation time. (b) To describe and discuss the VehicleSim features as a modelling tool in the helicopter field. It is mandatory to understand in detail the VehicleSim performance, if recent works such as dos Santos et al. [7], Misté and Benini [11] and Khaksar et al. [12] are able to be extended or complemented. (c) To study the impact that an accelerated and unbalanced main rotor has on the fuselage, in order to assess the capability of a multibody software to detect vibrations. This is carried out to ease the study of helicopter vibrations under complex mechanisms.

The outline of the paper is as follows: Section 2 presents the helicopter vibrations outlook. Section 3 provides a detailed description of the modelling process done in this work. Section 4 describes the modelling tool used: VehicleSim. Section 5 studies vibrations that appear on the fuselage when the main rotor speed is accelerated. Finally, Section 6 summarizes the main conclusions.

## 2. Helicopter vibrations outlook

The helicopter is designed to perform complex maneuvers that the fixed wing aircraft is not able to carry out, as for example the rescue operations, which some case can be executed in steep mountains, adverse sea conditions, etc. It is well known that a significant hurdle on the development of the rotorcraft progress is the vibration which retards the advances in the occupant's comfort and safety, among others. The vibration has an impact in the on board instruments and it can produce failure in the structural and non structural components [3,7]. The helicopter rotor blades are a relevant structural element, the damages on the blades would able to generate the loss of performance or even disastrous incidents. For a blade, these failure can cover, for instance the blade unbalance and impact damage, among others. As a consequence of this, the helicopters require to be periodically monitored. Nowadays, the vibration is being considered at design stage in order to reduce the costs i.e., it is needed to assess the vibration primarily. So, there is an increasing demand to establish the vibration impact on the helicopter structural components [6,12].

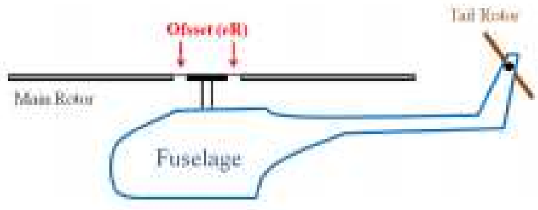


Fig. 1. Helicopter model with "offset" flap hinge indicated.

### 2.1. Flap and lag hinges features

The flap hinge allows the blade to rotate in a plane containing the blade and the shaft, of the disc plane, about either the actual flap hinge. The flap angle is commonly represented by $\beta$ and considered to be positive for upward blade motion. The flap hinge is more frequently designed to be at a short distance from the centre line. This distance is known as "offset" flap hinge (see Fig. 1). The flap motion is the result of the constantly changing balance between lift, centrifugal and inertial forces allowing the blade to drop when the rotor is at rest. In Fig. 2(a), an articulated rotor with a flap hinge offset from the centre of rotation by a distance eR is taken into account. Such an arrangement is usually mechanically simpler than one with no offset, and it has a favourable influence on the helicopter handling qualities.

A blade which is free to flap, experiences large Coriolis moments in the plane of rotation and a further hinge (called lag) is provided to relieve these moments. This degree of freedom produces blade motion on the same plane as the disc. The lag angle is represented by $\xi$ and it is considered to be positive when opposite to the direction of rotation of the rotor, as produced by the blade drag forces (see Fig. 2 (b)) [24,25].

### 2.2. Sources of vibration

Vibrations must be study in order to detect their main frequencies. This information can be used to design vibration control methods for helicopters. Due to the reduction of helicopter vibrations has traditionally been a cumbersome task to achieve. In a rotorcraft system there are many sources of excitation that introduce forced vibrations. Such sources include the main and tail rotors, the transmission shafts, the engine, etc. The primary forced vibration source is the main rotor with the hinged blade system. Blade displacement relative to all the hinges are also a source of vibrations. Vibrations from the main and tail blades are transmitted through the hubs. All parts of the helicopter are subjected to forced vibrations, however the amplitude of these vibrations differs. Its magnitude depends on the structure stiffness, the close-

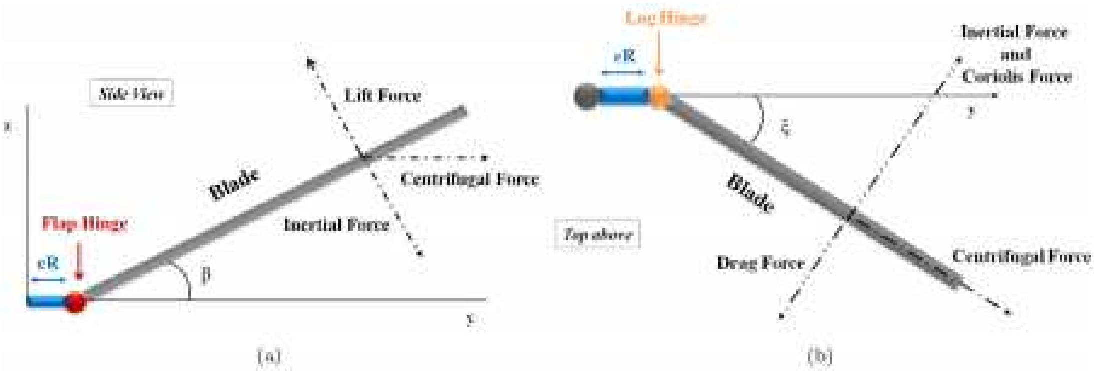


Fig. 2. (a) Side view of a flap hinge with offset *eR*. (b) Top view of a lag hinge with offset *eR*.

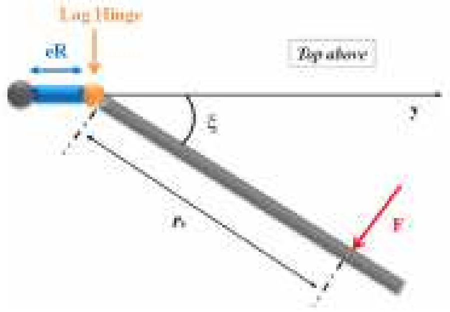


Fig. 3. Sketch of the force applied on the blade with a lag hinge.

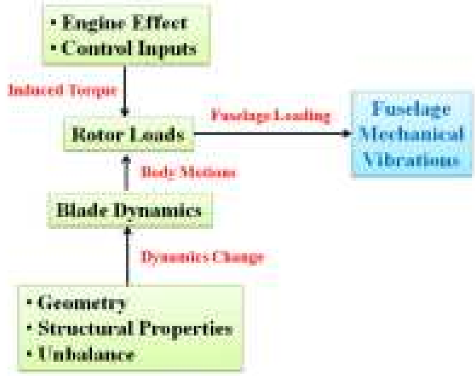


Fig. 4. Functional block diagram of helicopter vibrations.

ness of the exciting forces as well as their magnitude and points of application [24].

An additional vibration source in helicopters comes from rotor unbalance. The unbalance is a rotating force, which origin could be generated by blades mass unbalance or geometric asymmetry in their distributions. The last one could be originated by unequal the errors in geometry of articulation and unequal damper settings, among others. The corresponding responses depend on rotor mountings [26]. The vibration at the flap hinge should be taken into account for certain offset (eR). Because if the offset flap hinge is large, secondary vibrations will appear and they will be transmitted to the fuselage. In addition, when the offset is reduced, the hub receives its effect as well [27].

The blade motions around the lag hinge are essential in vibration systems. Its effect is drag variation that causes displacements around this hinge. In this scenario is suitable to employ a scheme of the blade replaced by centrifugal force acting along the blade axis, see Fig. 3. Therefore, the impact of main rotor lag hinge vibration on the fuselage should be also considered.

### 2.3. *Helicopter vibrations and simulations*

It is fundamental that the inherent helicopter vibrations are not only tackled in the conceptual design stages as the modifications, rectifications and continuous monitoring should be taken into account in successive stages. There are two types of helicopter vibrations. The unavoidable that cannot be eliminated and they are able to be minimized only. The other vibrations are derived of the imbalances associated to the blade trajectory as well as the individual blade mass imbalance. There are five main manner to diminish the vibration level, how are the improved blade design, the absorbers, the isolators, the fuselage dynamics optimizations and finally the reduction of aerodynamic excitation [3].

The simulation of dynamical vibrations and the corresponding analysis on a helicopter under certain operational conditions such as main rotor acceleration, it is a modelling task that can aid to detect technical failure and damage on its structure. The most common vibration analysis technique is the spectral analysis. This tool has shown to be relevant for the detection and the diagnosis of faults in rotating systems such as the rotorcraft, see [20,21]. The frequencies of vibrations generated by different components can be determined; thereby, a change in vibration level within a particular frequency band can be related to particular system component. As a consequence of this, an analysis of the associated vibration levels at different frequency bands is able to provide an indication of the nature of a fault or unbalance on the system components [6]. These diagnostic capabilities are fundamental to carry out the modelling and simulation of a helicopter in order to understand its performance properly.

As it can be seen, the condition monitoring and fault diagnosis of rotor system based on vibration signals are important as these systems are more and more complex due to the requirement of study the schema of varying angular speeds and dynamic loads. A typical target in vibration signal processing is to derive a representation in which certain features are displayed explicit. The most noteworthy and fundamental variables in signal processing are frequency and time [22].

Taking into account this considerations, it is clear that additional approaches are needed to simulate and study helicopter mechanical vibrations when accelerations are acting on the main rotor in form of engine effect and control inputs in matching with unbalance, structural properties and geometric configuration of the blades, see Fig. 4. In simulations of rotor dynamics, the blade elasticity should be considered, although certain studies was able to conduct using a rigid blade assumption [23].

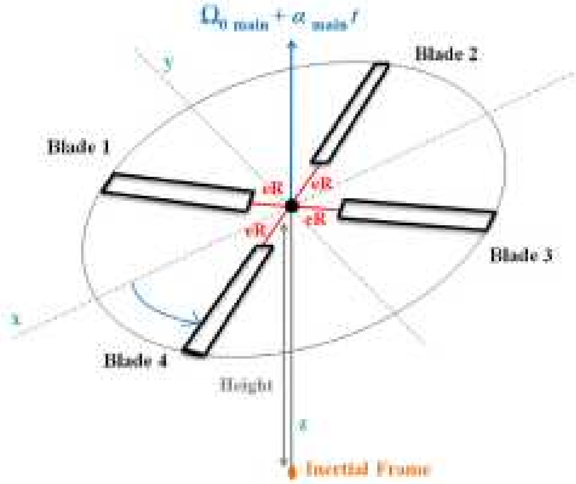


Fig. 5. Main rotor showing the spatial configuration in connection with inertial frame.

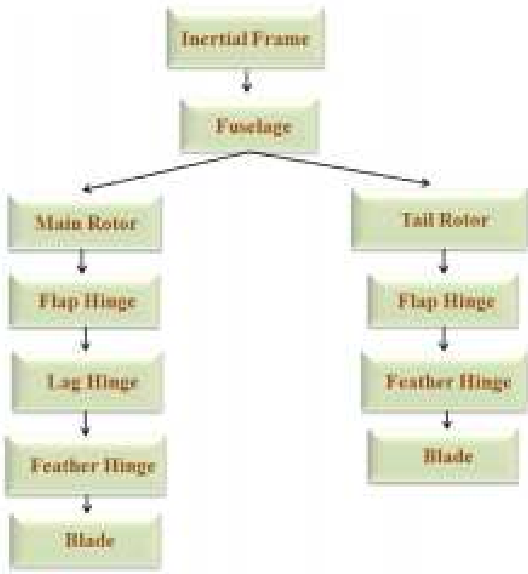


Fig. 6. Body structure diagram of the conventional model helicopter. Both main and tail rotor in this diagram contain one blade element only due to space restrictions, but the model can contain as many blades as needed.

## 3. Modelling

The main aim of this section is to describe the modelling process for implementing the helicopter model. The rotating systems have been studied and analysed by formulations and software tools that intrinsically take into account the reference rotation motion of the system. Such applications may be efficient and effective, however may present lack of generality. It has to be considered that the rotating systems are characterized by the non negligible angular motion which they are subjected to. The process of modelling is carried out under two premises: (a) To program a single code in VehicleSim and (b) To design a simulation tool that follows the current requirements fix by the helicopter vibration analysis (see Fig. 4).

### 3.1. General structure of the helicopter

A rotorcraft is able to be modelled in several manners; one of them is the combination of different interacting subsystems. Thus, a full helicopter dynamic model is taken into account as multibody system with several subsystems and constraints between the different degrees of freedom. The following considerations are done according to the physical structure of the helicopter (see [4]):

- The helicopter has the conventional configuration i.e., main rotor in combination with a tail rotor. Both systems are mounted on the fuselage. The model has been set up without empennage, see Fig. 1.
- The main rotor consists of four equally spaced blades joined to a central hub. The blades have free motion in and out of the plane of the disc; this is allowed by the inclusion of hinges, see Fig. 5.
- The tail rotor consists of two equally spaced blades joined to a secondary hub.
- The blades are rigid in both rotors.
- The rotor's angular speeds are constant, and a proportional ratio exists between them. The axis of rotation of the tail rotor is transverse to the main rotor's axis.
- The main rotor hinges allow for three degrees of freedom: flap, lag and feather motions.
- The tail rotor hinges allow for two degrees of freedom: flap and feather.
- Feather-flap coupling is considered in the tail rotor analysis.
- The helicopter's main body has six degrees of freedom. Three translations along the $(X, Y, Z)$ axes and three rotations around the same axes.
- The fuselage loads are obtained as the outputs of their corresponding translational and rotational degrees of freedom.

VehicleSim as well as its methodology have been also employed to model unmanned aerial vehicle (UAV) helicopter dynamic models (see [4,20]). In those cases, the rotorcraft features and geometry were different. Thereby, this software package as well as the developed model can be applied to other types of helicopter as UAV.

### 3.2. Helicopter modelling

The system modelled consists of three subsystems: fuselage, main rotor and tail rotor, see Fig. 1. The multibody system is subdivided into its constituent bodies for the purpose of writing the VehicleSim code [28]. The bodies are arranged as a parent/child relationship as shown in Fig. 6.

VehicleSim Lisp is a computer program that allows to model, to simulate and to derive symbolic equations of motion for mechanical systems composed of multiple rigid bodies. The inertial properties of the rigid bodies as well as the geometric that conform the system are provided as inputs. Forces and torques among the different model's component are able to add acting on the corresponding bodies. Therefore, it is convenient to include as first body in the code the fuselage. It is implemented as the child of the nominal reference frame. The fuselage is located at the origin of the inertial coordinates system and it is the parent of both the main and tail rotors. The main rotor rotates around its vertical axis, $Z$ axis. The main rotor is the parent of the flap hinges that rotates around the corresponding $X$ axis, each lag hinge is the child of the corresponding flap hinge. The lag hinges rotate around the $Z$ axis. The feather hinges are the child of the lag hinges. Each feather hinge rotates around the $Y$ axis. Finally, a blade is added to the program

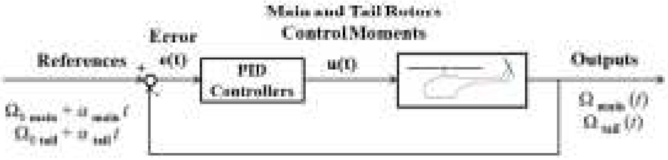


Fig. 7. PID helicopter rotors control.

**Table 1**
Helicopter model parameters [31,32].

| Parameters | Magnitude | Units |
|---|---|---|
| Helicopter mass | 2200 | kg |
| Main rotor blade mass | 31.06 | kg |
| Tail rotor blade mass | 6.21 | kg |
| Fuselage-main rotor vertical distance | 1.48 | m |
| Fuselage-tail rotor longitudinal distance | 6.00 | m |
| Fuselage-tail rotor vertical distance | 1.72 | m |
| Main rotor blade length | 4.91 | m |
| Tail rotor blade length | 0.98 | m |
| Main rotor angular speed | 44.40 | rad/s |
| Tail rotor gearing | 5.25 | – |

structure as the child of each feather hinge. The tail rotor is built up following this same parent/child structure. Additional data parameters such as masses, inertia matrices, coordinates of the centre of masses, the allowed rotations and translations of each body, which conform the dynamical system, can be described in a sequential manner along with the rigid bodies [29].

### 3.3. Main and tail rotors speed modelling

The main rotor angular speed makes use of a PID controller in order to regulate the speed according to omega (Ω), following a desired value (or time varying reference). An acceleration value is introduced to reach the prescribed rotational speed, gradually. This is dictated by the expression:

$$\Omega = \Omega_0 + \alpha t \quad (1)$$

where $\Omega_0$ is the initial main rotor angular speed, $\alpha$ is the main rotor angular acceleration and $t$ is the time. The input for this controller is the error between the actual rotor speed at each time step of the simulation interval and the prescribed rotational speed. The output of the PID controller is introduced in the model as a torque applied between the fuselage and the main rotor, see Fig. 7.

The tail rotor angular speed is proportional to the main rotor angular speed [4,31] and this is proportional the value of the tail rotor gearing, see Table 1. This angular speed is implemented in parallel way to the main rotor speed using a controller as well. The engine's action on the tail rotor is modelled as a torque applied between the fuselage and the tail rotor [30].

The model is implemented with these PID controllers due to their suitability to be modelled in VehicleSim. In this way, it is not required to employ further complex approaches. These controllers accomplish the objective set by the authors. In order to tune the controllers' gains, any PID tuning software has not been used. This procedure has been carried out manually. VehicleSim allows from the browser to change the numerical values of the parameters, if these have been defined in symbolic form on the code. In this way, the tuning is eased due to every execution from the browser provides swiftly the simulation results, allowing to evaluate the response to the error between the corresponding actual rotor speed and the prescribed rotational speed. The analysis of this error and the user decision making are essential to reach the required calibration.

VehicleSim does not generate or induce by itself any controllers' gains data. The user is who defines the procedure to follow i.e., if the program provides any information in this subject matter, it is because the user must establish the proper work environment. In order to tune the numerical values of the controllers' gains, external knowledge from other software platform or helicopter model has not been considered. The modelling process and the calibrations carried out by the authors, have led to an appropriate tuning of the controllers as well as a stable response into VehicleSim. As a result, if the acceleration is presented on the main rotor the proportional gain shows a numerical value upper to the derivative and this displays a value greater than the integral gain. Thereby, the gain numerical values have been determined using VehicleSim only.

According to Ren et al. [40] a linear model that approaches a particular nonlinear helicopter system is able to be achieved, if this performs around an operating point and the signals involved are small. Nevertheless, the control laws based on the linearised helicopter dynamics do not show global applicability as these only display desirable behaviour around an operating point. However, this approach is not considered in this work and the helicopter model is not tested at selected operating points.

### 3.4. Dynamics control

The torques and the dynamic loads do have an impact on the vehicle's stability. As a consequence of this, the helicopter trim control is a fundamental task that has to be tackled with special attention in the helicopter model. The coordinates in the inertial frame are ($x$, $y$, $z$), Euler angles ($\theta$, $\phi$, $\psi$) (roll, pitch, yaw), linear velocities ($\dot{x}$, $\dot{y}$, $\dot{z}$) and angular velocities ($\dot{\theta}$, $\dot{\phi}$, $\dot{\psi}$) in the body coordinate frame.

Several controllers on the translational and rotational degrees of freedom must be also incorporated. Thus, the helicopter's translational position control will be restored as well as the angular position, being this an essential step in the study and analysis of vibrations.

For stability purposes, the error between the reference and the actual states must be measured at each time step of the simulation. The outputs of these controllers require to be applied between the fuselage and the inertial frame to obtain an adequate action control. For example, in order to control the helicopter's position and displacement on the Y axis, the lateral position prescription for the fuselage's position has to establish in order to represent this. It provides the reference value for the lateral position; it allows to describe the origin of the reference system in the space. The output of this controller represents an applied force at the fuselage's centre of mass. Thus, the required lateral position control is obtained. Both longitudinal and vertical position controls were also modelled equally to this lateral position control.

In order to control the helicopter's roll degree of freedom, a PID controller is added. The input is the difference between the actual and desired fuselage's roll position. A reference value is defined at the beginning of model script. The output is a torque applied between the fuselage and the inertial frame. Pitch and yaw control are modelled similarly. As it can be seen, the rotorcraft dynamic model is implemented using PID controllers, due to their features allow to design an embedded simulation code in VehicleSim without requires additional software actions. Furthermore, this control approach is suitable enough to accomplish the authors objectives.

## 4. VehicleSim operation

VehicleSim is the main software package used in this work due to their advantages, for example, the automated equations provide an accurate representation of the complex system's dynamics and these are derived by VehicleSim, being no necessary to calculate

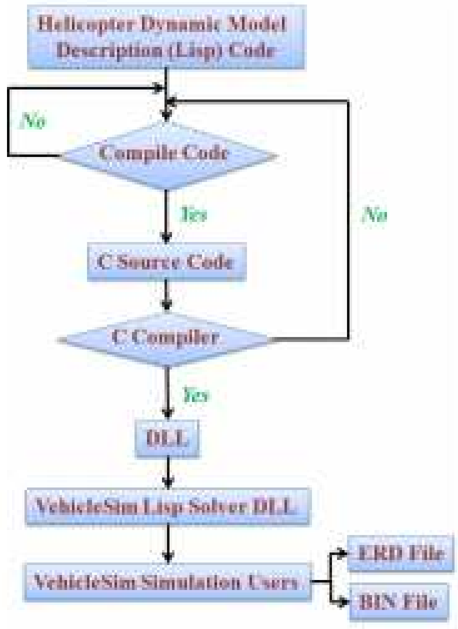


Fig. 8. Flow chart of VehicleSim simulation procedure.

these by hand (often this procedure is prone to errors). In addition to this, the execution time is diminished due to its software engineering features.

VehicleSim solvers on Windows are compiled as dynamically linked library (DLL) files with a standard VehicleSim application program interface (API), which is able to work with different simulation environments such as VehicleSim browser and Matlab. It is accessible by the user the source code generated by VehicleSim Lisp.

### 4.1. Overview of VehicleSim lisp

VehicleSim Lisp derives the equations of motion for a multibody system in symbolic form and a C source code is generated such that this program will solve the equations numerically to simulate the performance of the system represented by the model.

The symbolic equations obtained by VehicleSim Lisp are able to view and use with other software packages such as Word or Matlab. This is not a full simulation system as it is able to determine equations, however it does not solve them. As a consequence of this, a C compiler is required to compile the source code generated for a VehicleSim solver program and the DLL solvers are built up [29].

The main goal of each VehicleSim solver is to compute time histories of the system's variables, this is, the positions, speeds and accelerations of the bodies conforming the system and all user created variables. These time histories are stored in a binary data file with the extension BIN. The data in a BIN file are organized by variable name and sample number. A companion file, with extension ERD, documents the layout of the BIN file. The ERD header file also contains labelling information for each variable. Data processing programs for ERD and BIN files derive the information required from the ERD file (see Fig. 8) [33].

### 4.2. VehicleSim and state variables

The state variables for a multibody system as VehicleSim are separated into two sets: generalized coordinates and generalized speeds. In VehicleSim environment, the term "state variables" generally refers only to variables that are defined by differential equations. However from the user perspective, the set of state variables also established variables which are not determined by differential equations, but whose values are needed to fully define the current state of the model. This software introduces the state variables required to describe the moving reference frames, and employs them as needed to work out mathematical expressions of variables that represent the equations of motion of the system.

VehicleSim Lisp is able to obtain expressions for the absolute coordinates of any point located on any mechanical part using the generalized coordinates and dimensional parameters. The generalized coordinates are the variables that involve translational and angular displacements. The set of generalized coordinates is established such that it is feasible to reconstruct the position of any point in any part in the system. Furthermore, a set of generalized speeds complements the set of generalized coordinates, by adding the ability for VehicleSim Lisp to calculate the velocity vector of any point located on any part in the multibody system.

The definition of state variables can be controlled, these are introduced automatically when the command `add-body` is employed to established a body that is able to move relative to its parent. The equations of motion for a system involve a minimum number of coordinates and a speed variable is introduced automatically with each coordinate. One generalized coordinate is inserted for each degree of freedom of the new body relative to its parent, and the coordinates are the amplitudes of the permitted displacements. The speed variable is defined as the derivative of the coordinate, except for the following three cases [29]:

- A body with three translational degrees of freedom relative to its parent has three translational speed variables defined as scalar measures of the absolute velocity of the body mass centre.
- A body with three rotational degrees of freedom relative to its parent has three rotational speed variables defined as scalar measures of the absolute rotational velocity of the body.
- A body restricted to planar motions, with two translational degrees of freedom has the translational speeds defined as scalar measures of the absolute velocity of the body mass centre.

### 4.3. Numerical solution

VehicleSim-Browser is incorporated to VehicleSim package as the solver program. It calculates the output variables at intervals of time as the simulation is being done. The time history of the output variables is computed by solving the dynamical equations of motion containing the state variables. There are four types of computation methods which could be used by in a VehicleSim solver program: (a) simple arithmetic statements. (b) Numerical integration of a set of ordinary differential equations. (c) Solution of a set of simultaneous linear algebraic equations. (d) Solution of a set of simultaneous nonlinear algebraic equations.

### 4.4. Multibody modelling and methodology

VehicleSim Lisp usually follows the modelling sequence as shown in Fig. 9. VehicleSim commands are employed to describe the components of a multibody system in a parent/child relationship in accordance with their physical constraints and joints. As it can be seen in Fig. 9, the commands categorize in sequential way the bodies that make up the system, additionally the corresponding physical values are incorporated. A VehicleSim program begins with an inertial reference frame with a fixed origin selected by the user, and a trihedron with their directions is established. As new bodies are incorporated to the system, having freedoms relative to the inertial reference frame, local origins and axes are defined.


**Fig. 9.** VehicleSim commands main sequence.

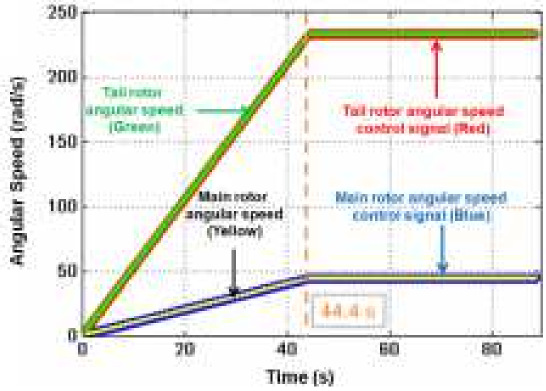


**Fig. 10.** Rotor angular speeds. Yellow '-', the main rotor angular speed. Green '-', the tail rotor angular speed. The control signals needed to achieve them are shown on both cases. Blue '"', the reference signal for the main rotor speed. Red '"', the reference signal for the tail rotor speed. (For interpretation of the references to colour in this figure legend, the reader is referred to the web version of this article.)

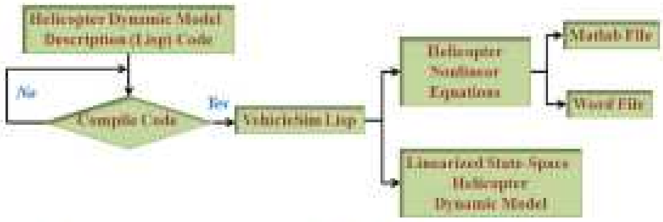


**Fig. 11.** Flow chart of VehicleSim simulation procedure for the state-space.

Generally, at the head of a VehicleSim program there are determined commands that are used to reset the system. For example, to define the gravitational field, to select the unit system to be used and the possible linearization of equations of motion, among others. If these matters are not overtly selected, there is a configuration file which the user is free to access and where the default settings are established.

The code is able to transform from local coordinates to global ones and vice versa. Points specified globally are conveniently employed to determine points in bodies. The body fixed points coincide with the corresponding global points, fixed in the inertial reference frame, when the system is on its nominal configuration. Most points are fixed in bodies, however a point may be defined as moving with its location in a body defined by its specified coordinates. This is suitable for describing time varying contact points between two bodies [29].

## 5. Results: helicopter simulation model

The main rotor vibrations are transmitted to the fuselage and it will display several vibration modes. Depending on which mode is excited, the amplitude and frequency of the vibration will change, which affects to the feasible performance and the safety of the helicopter [34,35]. There are a number of secondary sources of vibrations which should also be taken into account, for example, the flap hinges offset causes rolling and pitching vibrations that are transmitted to the fuselage. In this section, these are studied under the influence of an accelerating helicopter main rotor. The main and tail rotor angular speeds performance are presented and a frequency domain study is carried out for the flap and lag modes on the main rotor. Finally, the impact of the lag hinge is studied for an structural unbalance on the main rotor.

### 5.1. *Main and tail rotor speeds*

In order to study the vibrations appearing on the fuselage, the capability of the helicopter model to develop accelerations on both rotors is checked. The rotor angular speeds are generated without immediately response. So, these start to rotate from rest up to a nominal value (44.4 rad/s) and (5.25·44.4 rad/s), respectively. As it was mentioned in Section 3.3, these accelerations are able to carry out using the PID controllers implemented in VehicleSim, their corresponding numerical values are defined at the beginning of the VehicleSim Lisp code. The initial rotor angular speeds are zero and they are increased with an angular acceleration of 1 rad/$s^2$, which allows to reach the nominal angular speed in 44.4 s. Once the desired speed reference values are reached, the accelerations are set to zero and the angular speeds remain constant at the prescribed values as Fig. 10 shows. In both rotors, the corresponding angular speeds follow the control signal required to obtain the rotating speeds.

### 5.2. *Frequency domain study: main rotor flap and lag modes analysis*

The state space method provides the solution of the small perturbation rotorcraft equations of motion. In fact, VehicleSim derives in form of a Matlab file the linearised state-space model in symbolic form. Moreover, VehicleSim generates the model's linearised and nonlinearised equations of motion in form of differential equations, see [4,36]. Most software destined to solve problems in modern control, must ensure that the helicopter equations of motion are properly assembled, before a solution is calculated using these tools [37]. The determination of the structural response as well as the modal frequencies are fundamental to design rotating components such as helicopter blades [38,39]. Taking into account these considerations and due to the flap and lag degrees of freedom have a relevant role in this work, these are studied by using frequency domain. VehicleSim allows to carry out this type of study and the user can focus the analysis on selected parts of the system. The assessment of these parts does not implicate that the helicopter model is simplified. This is done to check the proper implementation of them.

VehicleSim generates the linearised model that contains the symbolic state space A, B, C, D matrices for linear analysis, see Fig. 11. In addition to this, the nonlinear equations of motion on each case are obtained in C code, and this is used to generate states' time histories, see Fig. 8. In order to obtain the eigenvalues/eigenvectors of the state matrices, the state's time histories are imported from the nonlinear model into the symbolic linearised model matrices. As a consequence of this and in order to study the dynamic behaviour around the equilibrium position for the main rotor flap and lag modes, the dynamic equations of motion are obtained and a frequency domain analysis is carried out. According to this, if the equilibrium conditions must be achieved, the accelerations are not activated on the rotors.

The flap linear state equation is obtained in VehicleSim as:

$$\ddot{\beta}\left(I_{blx} + m_{bl}y_{bl}^2\right) = -m_{bl}\Omega^2 y_{bl}(eR + y_{bl})\beta - \Omega^2\left(I_{blz} - I_{bly}\right)\beta - k_{fj}\beta \tag{2}$$

where $I_{blx}$, $I_{bly}$, $I_{blz}$ are the corresponding main rotor blade moments of inertia around $x$, $y$ and $z$ axis, respectively. $m_{bl}$ is the main rotor blade mass. $y_{bl}$ is the main rotor blade's centre of mass. $k_{fj}$ is the main rotor flap hinge spring stiffness.

This can be written in matrix form:

$$\begin{pmatrix} \dot{x}_1 \\ \dot{x}_2 \end{pmatrix} = \begin{bmatrix} 0 & 1 \\ F & 0 \end{bmatrix}\begin{pmatrix} x_1 \\ x_2 \end{pmatrix}$$

where $x_1 = \beta$, $x_2 = \dot{\beta}$ and F is equal to:

$$\left[-k_{fj} - m_{bl}y_{bl}^2\Omega^2 - \Omega^2 eRm_{bl}y_{bl} + \Omega^2\left(I_{bly} - I_{blz}\right)\right] \Big/ \left(I_{blx} + m_{bl}y_{bl}^2\right) \tag{3}$$

By feeding the matrix elements with the corresponding physical parameters, the eigenvalues are obtained and found to be: $\lambda_{1,2} = 0 \pm 48.8564i$ where the complex part of $\lambda_{1,2}$ is the flap natural frequency, 48.8564 rad/s slightly above the main rotor angular speed, as this simulation corresponds to the case of there is a flap spring $k_{fj} = 46772$ Nm/rad, and offset $eR \neq 0$.

$$\begin{pmatrix} \dot{y}_1 \\ \dot{y}_2 \end{pmatrix} = \begin{bmatrix} 0 & 1 \\ H & G \end{bmatrix}\begin{pmatrix} y_1 \\ y_2 \end{pmatrix}$$

where $y_1 = \xi$, $y_2 = \dot{\xi}$:

$$H = -\left(k_{fj} + eRm_{bl}\Omega^2 y_{bl}\right)/\left(I_{blz} + m_{bl}y_{bl}^2\right) \tag{4}$$

and

$$G = -d_{lj}/\left(I_{blz} + m_{bl}y_{bl}^2\right) \tag{5}$$

$d_{lj}$ is the main rotor lag hinge damping coefficient.

In this case, the eigenvalues of the matrix are: $\lambda_{1,2} = -0.5448 \pm 35.3776i$. The natural lag frequency is 35.3776 rad/s and the system's damping is provided by the real part of $\lambda_{1,2}$, these values agree with the expected.

- Root locus

The linear approximation allows to shed some insight on the complex motion of the blade. The linear natural modes of the blade are analysed from the stability point of view. A layout of the uncoupled flap and lag modes is represented on the complex eigenvalues plane in Fig. 12(a). This has been carried out for the helicopter model operating at equilibrium conditions i.e., the main and tail rotors are given in the form of a constraint and the blades have initial flap angles $\beta_0 = 0$, these do not vary independently their corresponding displacements. In this way, the rigid blades fluctuations are established and the conditions of dynamic equilibrium are achieved. The main rotor angular speed is 44.4 rad/s, the tail rotor angular speed is zero and gravity is not considered. In order to determine the eigenvalues/eigenvectors, the state's time histories are extracted from the nonlinear model into the symbolic linearised model matrices at each timestep of the running interval. The result is plotted as a root locus diagram in Fig. 12(a). As shown, the lag mode is well damped ($d_{lj} = 349.58$ Nms/rad). The flap mode in this case does not have a damper, therefore its mode it is located on the imaginary axis i.e., the mode is marginal stable.

A typical layout of the uncoupled flap and lag modes is presented by Padfield [31]. It shows how the flap modes are well damped and located far into the left hand side of the plane. In contrast, the lag modes are often weakly damped, even in the presence of mechanical dampers, being more susceptible to the instability. This result is considered to do a comparison and to validate the linear natural modes of the blade. As a consequence of this, a damper of 500Nms/rad is included on the flap hinge and several simulations are carried out. The result is displayed in Fig. 12 (b), wherein the imaginary axes have been normalized i.e., the corresponding numerical values have been divided by the main rotor angular speed. As shown, the flap modes are well located into the left hand side of the plane. Parameter differences aside, Fig. 12 (b) clearly shows an agreement with the expected performance [31]. Nevertheless, the frequencies of the modes are slightly different due to the aerodynamic load was considered in reference [31] and aerodynamic load aids to increase the frequency.

### 5.3. Simulations for vibration generation

The main goal of this subsection is to test the performance of the embedded code, as a tool of helicopter structural features analysis. The main rotor is not a simple vibrating system as it consists of several rotating bodies linked by hinges. Its continuous state of rotation and its vibration motion are superimposed on a rotation. Other non-uniformities, equivalent to the rotating force, can be generated and they are able to produce a difference in centrifugal force. As a consequence of this, the blades rotate under the influence of an unbalance of forces. This is the most frequent cause of unbalance in the helicopter rotors. It should be borne in mind that the centrifugal restoring constraint in the lag motion of an articulated rigid blade around a lag hinge is weaker than the flap displacement [26].

#### 5.3.1. Offset flap hinges' vibrations

Several simulations are done for two different offset values. The simulations are run for several initial flap angles on each blade to insert an additional small unbalance on the main rotor blades, thus the corresponding blades flap stiffness springs generate diverse reaction forces. The unbalanced masses on the main rotor, vacuum and no gravity are also considered. The lag degree of freedom is not activated, neither the tail rotor angular rotation. As it can be seen, this simulation tool permits to select various helicopter configurations independently, which done especially useful this approach.

Six degrees of freedom are presented on the helicopter's fuselage. The mass of the blades on the main rotor are assumed to be slight unbalance: $m_{bl1} = 31.06$ kg, $m_{bl2} = 31.26$ kg, $m_{bl3} = 29.96$ kg and $m_{bl4} = 31.16$ kg. The flap hinge offset for the four blades is the same, $eR = 0.01$ m. The corresponding initial flap angles are selected as $\beta_1 = 0.0175$ rad, $\beta_2 = 0.075$ rad, $\beta_3 = 0.0675$ rad and $\beta_4 = 0.0875$ rad. The collective and cyclic feather angles are zero in the main rotor. The simulation time is 44.4 s, the initial angular speed on the main rotor is $\Omega = 0$ rad/s and the main rotor has an angular acceleration of 1 rad/s$^2$. This stage should be suitable to assume structural unbalance in the helicopter configuration, which will allow to assess the capability of the code as a detection tool of vibrations. With this experimental set up, simulations are performed and the vibrations appear on the fuselage, ready to be analysed. These conditions are just taken as example, being possible to produce fuselage vibrations with other several combinations.

The study of these vibrations is done by analysing spectrograms derived when a short time Fourier transform is applied (STFT). The

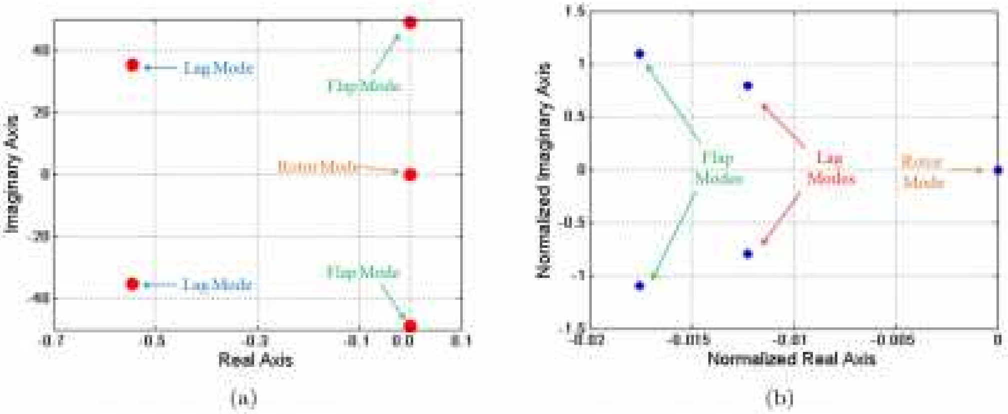


**Fig. 12.** (a) Root locus for flap and lag modes on the main rotor. (b) Root locus plot flap and lag modes obtained by VehicleSim with damper fitted in the flap hinge. (Note normalized in both axes).

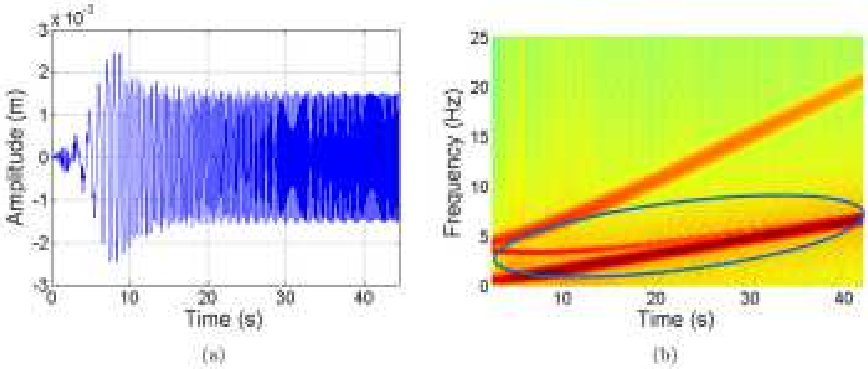


**Fig. 13.** (a) Fuselage oscillations on the *X* axis for $eR = 0.01$ m. (b) Spectrogram of the vibrations shows various frequencies varying between 0–7 Hz, 4.5–21 Hz and 3.5 Hz, respectively.

STFT of a signal $X(t)$ is able to be determined as:

$$S_x(t, \omega) = \int_{-\infty}^{\infty} X(\tau) h(\tau - t) e^{-j\omega\tau} d\tau \tag{6}$$

$X(t)$ is the signal under study, and $h(t)$ is a finite support window function. The properties of the window function $h(t)$ have a significant effect on the STFT result and should be carefully selected. The spectrograms of the signals (states' time histories) have been worked out with an overlapping of 99% to get a good compromise between time and frequency resolutions and a 44.4 seconds time window. The low and high frequency components were omitted, due to the size of the window, the spectrograms for the first and the last seconds are not able to be shown. However, the different frequencies can be clearly identified.

Fig. 13 shows the vibration and the spectrogram of frequencies on the fuselage *X* axis. As it can be seen, there are two predominant frequencies, the first is between zero and 7 Hz approximately and the second is observed between 4.5 Hz to 21 Hz. In addition to these, a third frequency is detected around 3.5 Hz, however this becomes equal to the first frequency at the end of the simulation time. The sources of these frequencies are the main rotor acceleration, the unbalance of masses and the different initial flap angles on the blades, respectively. The last one is detected due to the impact that the inertial and centrifugal forces generated on the root of the blades as the main rotor is accelerated.

A similar analysis is able to be done for the fuselage on the *Y* axis. The fuselage vibration and the spectrogram are plotted in Fig. 14. Two predominant frequencies are also identified, their values are between zero and 7 Hz, and 4.5 Hz to 21 Hz. Finally, a third frequency is detected around 3.5 Hz and after some seconds, this reaches the first frequency value at the end of the simulation. As shown, the *X* and *Y* axes are sufficient to evaluate the capability of this rotorcraft model as a detection tool of vibrations.

A second simulation must be done, in order to visualize the impact of the offset flap hinge on the fuselage in form of vibration, for an accelerated main rotor. The offset value is increased to $eR = 0.982$ m. The rest of the parameters and the initial conditions remain constant. The main purpose is to detect the impact of the secondary vibrations around the fuselage *X* and *Y* axes for a higher offset value. The vibrations and the frequencies spectrogram for the fuselage oscillations around the *X* axis are displayed in Fig. 15. The spectrogram shows three predominant frequencies, two of them were clearly observed for ($eR = 0.01$ m). However, a third frequency is detected between 3.5 Hz to 9 Hz until the end of the simulation time. Analogous results are obtained for the fuselage *Y* axis, see Fig. 16. So, it has shown the impact of the offset flap hinge on the fuselage for an accelerated main rotor.

As shown Fig. 15 (b) and Fig. 16 (b), for large flap hinge offset appears a third spectral component clearly (black lines mark). However if the offset is reduced, the previous spectral component matches with the main rotor frequency after some seconds, see Fig. 13 (b) and Fig. 14 (b).

### 5.3.2. *Lag hinge vibrations*

The main rotor lag hinge should be also taken into account in order to study its impact on the fuselage. Thus, the centre of mass of each blade is slightly modified. This generates an unbalance that adds a dynamic load on the main rotor. As a consequence of this, the vibrations on the fuselage should be sensed. The flap degree of freedom is not implemented due to the study is done for a pure lag hinge.

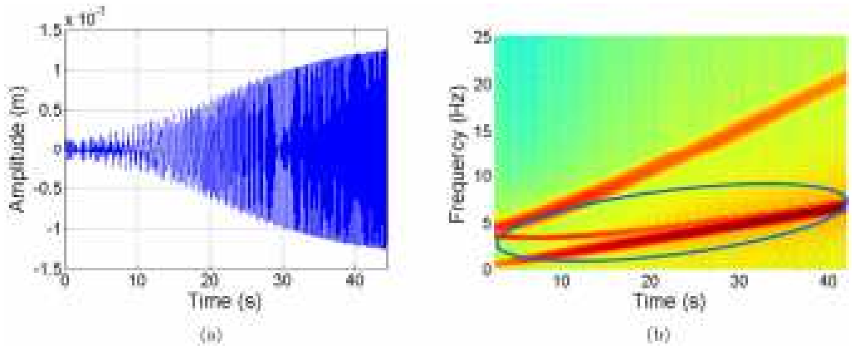


Fig. 14. (a) Fuselage oscillations on the $Y$ axis for $eR = 0.01$ m. (b) Spectrogram of the vibrations shows various frequencies varying between 0–7 Hz, 4.5–21 Hz and 3.5 Hz, respectively.

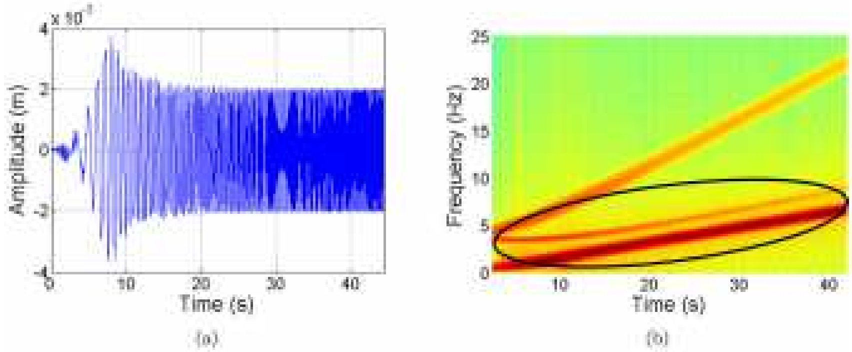


Fig. 15. (a) Fuselage oscillations on the $X$ axis for $eR = 0.982$ m. (b) Spectrogram of the vibrations shows various frequencies varying between 0–7 Hz, 4.5–22.5 Hz and 3.5–9 Hz, respectively.

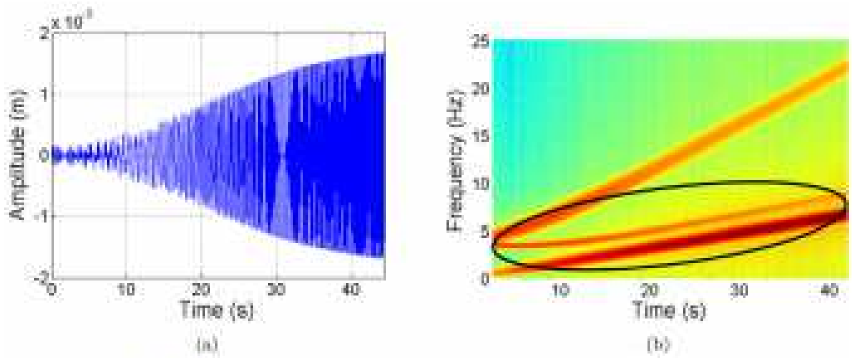


Fig. 16. (a) Fuselage oscillations on the $Y$ axis for $eR = 0.982$ m. (b) Spectrogram of the vibrations shows various frequencies varying between 0–7 Hz, 4.5–21 Hz and 3.5–9 Hz, respectively.

The following simulation stages are considered; the six degrees of freedom are allowed on the fuselage. The mass of the blades on the main and tail rotors are equally balanced. The centre of mass of the four blades on the main rotor are unbalanced as $y_{M1} = 2.9846$ m, $y_{M2} = 2.7846$ m, $y_{M3} = 2.8846$ m and $y_{M4} = 2.6846$ m. Collective and cyclic feather angles are zero in the main rotor. The tail rotor angular rotation is deactivated. The simulation time is 44.4 s, the initial angular speed is zero and an acceleration of 1 rad/s$^2$ is run. This configuration should be adequate to generate vibrations. Several other combinations could be chosen, however this one is provided to test the helicopter model capability as a tool in the rotorcraft design. The result is shown in Fig. 17. From the spectrogram a predominant component is detected on the fuselage $X$ axis, its value is between 0 and 7 Hz, approximately. A second frequency is observed around 7 Hz and 9 Hz, being its time interval 5 s, after this the signal disappears. Similar spectrogram is figured out for the fuselage $Y$ axis, being the result analogous see Fig. 18. The sources of these frequencies are the main rotor acceleration and the additional dynamic load produces by the unbalance on the blade centre of mass. The last one generates a force at the blade root that it is transmitted to the fuselage. When the main rotor angular speed achieves certain value, the slight unbalance has not any effect. Due to the blades are rotating uniformly among them and the corresponding main rotor angular speed cancels its impact.

A second simulation is carried out for the same conditions and parameters. Nevertheless, the unbalanced centre of mass is modified as follows $y_{M1} = 3.9846$ m, $y_{M2} = 1.7846$ m, $y_{M3} = 3.8846$ m, $y_{M4} = 1.6846$ m for the blade one, two, three and four on the main rotor, respectively.

From the spectrogram in Fig. 19, the fuselage oscillations around the $X$ axis displays a frequency which value is between 0 and 7 Hz, approximately. A second frequency between 6 Hz and 12 Hz is also observed, its interval of time is 10 to 26 s. In comparison to the previous results, it is clear that if the unbalance of blade centre of masses is increased, the frequency of vibrations ap-

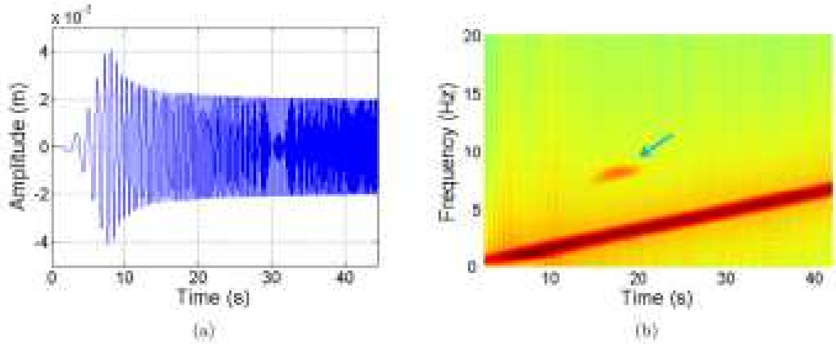


**Fig. 17.** (a) Fuselage oscillations on the *X* axis for $y_{M1} = 2.9846$ m, $y_{M2} = 2.7846$ m, $y_{M3} = 2.8846$ m, $y_{M4} = 2.6846$ m. (b) Spectrogram of the vibrations shows various frequencies varying between 0–7 Hz, 7–9 Hz, respectively. (For interpretation of the references to colour in the text, the reader is referred to the web version of this article.)

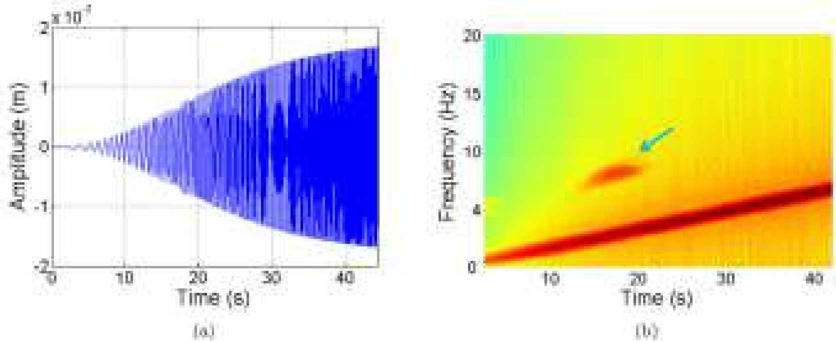


**Fig. 18.** (a) Fuselage oscillations on the *Y* axis for $y_{M1} = 2.9846$ m, $y_{M2} = 2.7846$ m, $y_{M3} = 2.8846$ m, $y_{M4} = 2.6846$ m. (b) Spectrogram of the vibrations shows various frequencies varying between 0–7 Hz, 7–9 Hz, respectively. (For interpretation of the references to colour in the text, the reader is referred to the web version of this article.)

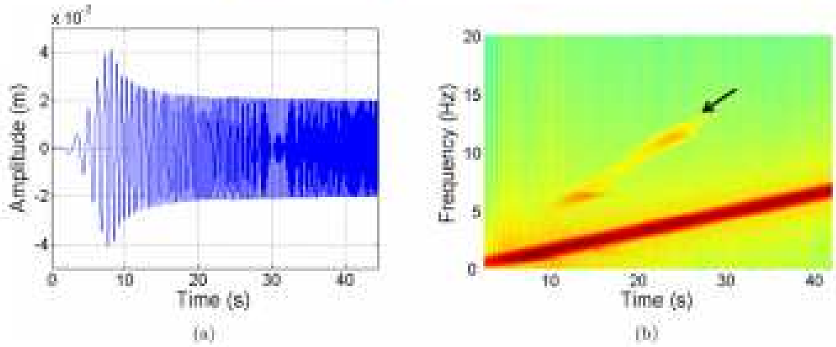


**Fig. 19.** (a) Fuselage oscillations on the *X* axis for $y_{M1} = 3.9846$ m, $y_{M2} = 1.7846$ m, $y_{M3} = 3.8846$ m, $y_{M4} = 1.6846$ m. (b) Spectrogram of the vibrations shows various frequencies varying between 0–7 Hz and 6–12 Hz. (For interpretation of the references to colour in the text, the reader is referred to the web version of this article.)

pearing on the fuselage also increases. This vibration is presented during certain period of time, after this disappears. The origin of each frequency is equal to the dealt with in previous case. However, there is a significant difference, when the unbalance of blade centre of masses has been raised, the spectral component associated to this, has shown that its impact is larger.

The vibration appearing around the fuselage *Y* axis is studied in similar manner. From Fig. 20, it is able to see a predominant frequency between 0 and 7 Hz approximately. A second frequency arises around 5–12 Hz, during the interval of time 10–26 s, after this the signal is vanished. The source of each frequency is analogous to *X* axis explained above.

As the main rotor is accelerated from 0 rad/s to 44.4 rad/s, there is an applied dynamic load causing a moment. This shows its effect until 21 rad/s approximately, as it is indicated in blue arrows (Figs. 17 (b) and 18 (b)). If the angular speed is greater than this value, the vibration disappears. On the other hand, if the unbalance of centre of masses is increased, the spectral components rise as well. The vibrations persist for a longer interval of time, see Figs. 19 (b) and 20 (b) (black arrows). So, the impact of the lag hinge has been observed on the fuselage due to the unbalance on blade centre of masses.

## 6. Conclusions

The rotorcraft modelling problems and their inherent nonlinearities are a cumbersome task, the multibody dynamics approach can shed light on these. Thus, this work presents a helicopter dynamic model which is capable to transmit perturbations from the main rotor to the fuselage in form of vibrations. The model has been implemented in VehicleSim, a program that allows to establish a system as a composition of several bodies and constrains by using a parental relationship structure. This software has been used because the system nonlinear equations as well as the state space matrices are derived, and the nonlinear dynamics couplings

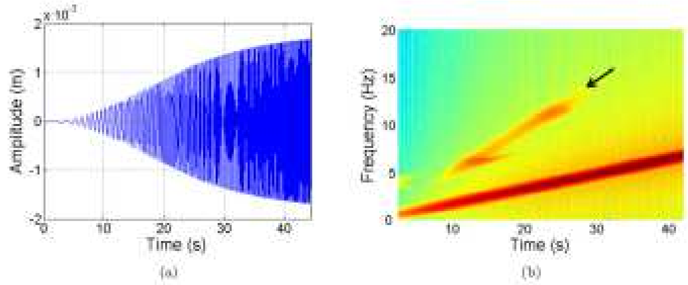


**Fig. 20.** (a) Fuselage oscillations on the Y axis for $y_{M1}$ = 3.9846 m, $y_{M2}$ = 1.7846 m, $y_{M3}$ = 3.8846 m, $y_{M4}$ = 1.6846 m. (b) Spectrogram of the vibrations shows various frequencies varying between 0–7 Hz and 5–12 Hz. (For interpretation of the references to colour in the text, the reader is referred to the web version of this article.)

are achieved. As a consequence of this, the VehicleSim implementation tasks have been dealt with.

In order to control the accelerated rotors angular speed, two PID controllers have been modelled. Due to it is the more straightforward control that it is able to be developed without required the use of external software in VehicleSim. This is a mandatory aspect, if an embedded code is programmed using this, exclusively. The approach is effective to accomplish the demanded objectives and to achieve some advantages such as the reduction of the compilation time as well as the code portability. In addition to this, the state space has allowed to study and validate the main rotor uncoupled flap and lag modes. This was done as the rotorcraft nonlinear equations of motion were obtained in C, the time histories were derived and the linearised state space model was generated in symbolic form as a Matlab file. In VehicleSim, a typical local stability study requires the importation of quasi-steady time histories from the nonlinear simulation to the symbolic linearised equations of motion. The mode shapes have been studied and the results evidenced good agreement with theoretical findings existing in the literature.

To study the vibrations appearing on the fuselage's roll and pitch axes, some parameters have been changed, such as the offset flap hinge, the blade centre of mass and the initial blade flap angle. Besides, an unbalance of mass on the main rotor blades has also been taken into account. The roll and pitch axes have been sufficient to assess the capability of the model as a detection tool of vibrations. Various tests were carried out to determine the impact that the offset flap hinge and the lag hinge have under the action of these conditions. In both set of simulations and doing use of the short time Fourier transform, the contribution of these hinges as sources of vibration were tested.

The authors expect to increase the complexity of the dynamical model in further works, as for example, including the blades flexibility. The study of the implementation the nonlinear controllers into VehicleSim is a task that must also be considered for future works. Nevertheless, the main goal of this work is to set up the basis of an embedded helicopter model code by using VehicleSim only, and to assess its capability to detect the impact of the vibrations on the fuselage. In summary, the work here presented provides a modelling method for the detection dynamic vibration in a helicopter model for an accelerated main rotor.

## References


[1] Leishman JG. A history of helicopter flight. Cambridge University Press; 2000.
[2] King SP. The minimisation of helicopter vibration through blade design and active control. Aeronaut J 1988;92(917):247-64.
[3] Kumar JS. Helicopter vibrations - a perspective. Int J Res Aeronaut Mech Eng 2016;4(6):50–63.
[4] Castillo-Rivera S. Advanced modelling of helicopter nonlinear dynamics and aerodynamics. School of Engineering and Mathematical Sciences. City University London. United Kingdom; 2015. Ph.D thesis. http://openaccess.city.ac.uk/13169/.
[5] Castillo-Rivera S, Tomas-Rodriguez M. Helicopter nonlinear aerodynamics modelling using vehiclesim. Adv Eng Softw 2016;100:252–65.
[6] Stupar S, Simonovic A, Jovanovic M. Measurement and analysis of vibrations on the helicopter structure in order to detect defects of operating elements. Sci Tech Rev 2012;62(1):58–63.
[7] dos Santos FLM, Peeters B, Van der Auweraer H, Góes LCS. Vibration-based damage detection for a composite helicopter main rotor blade. Case Stud Mech Syst Signal Process 2016;3:22–7.
[8] Zhou S, Shi J. Imbalance estimation for speed-varying rigid rotors using time-varying observer. J Dyn Syst Measure Control 2001;123:637–44.
[9] Zhou S, Shi J. The analytical imbalance response of jeffcott rotor during acceleration. J Manuf Sci Eng 2001;123(2):299–302.
[10] Zhou S, Dyer SW, Shin K, Shi J, Ni J. Extended influence coefficient method for rotor active balancing during acceleration. J Dyn Syst Measure Control 2004;126(1):219–23.
[11] Mistè GA, Benini E. Variable-speed rotor helicopters: performance comparison between continuously variable and fixed-ratio transmissions. J Aircraft 2016;53(5):1189–1200.
[12] Khaksar Z, Anavatti S, Shankar K, Ceruti A, Pratt H. The vibration impact determination of the helicopter structural components. MATEC web of conferences, vol. 95; 2017. doi:10.1051/matecconf/20179507027. 07027.
[13] Abaqus 6.12. Getting started with abaqus: interactive edition. Dassault Systemes 2012.
[14] Ceruti A, Liverani A, Recanatesi L. Improving helicopter flight simulation with rotor vibrations. In: Proceedings of the IMProVe 2011. International conference on innovative methods in product design. June 15th–17th, Venice, Italy; 2011.
[15] de Oliveira C G, Simpson DM, Nadal J. Lumbar back muscle activity of helicopter pilots and whole-body vibration. J Biomech 2001;34(10):1309–315.
[16] Kaptis IA, Valavanis KP. Linear and nonlinear control of small-scale unmanned helicopters. Volume 45 of the series intelligent systems, control and automation: science and engineering; 2011. p. 13–19.
[17] Chen M, Shi P, Lim CC. Adaptive neural fault-tolerant control of a 3-DOF model helicopter system. IEEE Trans Syst Man Cybern 2016;46(2):260–70.
[18] Cui Q, Lei Z, Chen M. Observer based backstepping control for a three degree of freedom model helicopter. In: IEEE Chinese guidance, navigation and control conference (CGNCC), Nanjing; 2016. p. 2299–304.
[19] Agneni A, Coppotelli G, Grappasonni C. Operational modal analysis of a rotating helicopter blade. In: Proceedings of ISMA2010 including USD2010; 2010. p. 3249–62.
[20] Marichal-Plasencia GN, Tomas-Rodriguez M, Castillo-Rivera S, Hernandez-Lopez A. Modelling analysis of vibrations in a UAV helicopter with a vision system. Int J Adv Rob Syst 2012;9:220. ISSN: 1729–8806
[21] Marichal GN, Tomas-Rodriguez M, Hernandez A, Castillo-Rivera S, Campoy P. Vibration reduction for vision system on board UAV using a neuro-fuzzy controller. J Vib Control 2013;20(15):2243–253.
[22] Dongfeng S, Liangsheng Q, Ming B. Instantaneous purified orbit: a new tool for analysis of nonstationary vibration of rotor system. Int J Rotating Mach 2001;7(2):105–15.
[23] Floros M, Johnson W. Advanced rotor aerodynamics concepts with application to large rotorcraft. In: American helicopter society aerodynamics, acoustics and test and evaluation technical specialists meeting. San Francisco, CA; 2002. p. 23–5.
[24] Johnson W. Helicopter theory. Princeton, NJ: Princeton Univ. Press; 1980.
[25] Magari PJ, Shultz A, Murthy VR. Dynamics of helicopter rotor blades. Comput Struct 1988;29(5):763–76.
[26] Shapiro J. Principles of helicopter engineering. Temple Press Limited; 1955.
[27] Payne PR. Helicopter dynamics and aerodynamics. Sir Isaac Pitman & Sons, LTD; 1959.
[28] http://www.carsim.com/; 2017 [accessed 31.07.17].
[29] Mechanical Simulation Corporation. Vehiclesim solver programs reference 1046 manual. Mechanical Simulation. http://www.carsim.com; 1997–2008 [accessed 31.07.17].
[30] Masarati P. Computed torque control of redundant manipulators using general-purpose software in real-time. Multibody Syst Dyn 2014;32(4):403–28.
[31] Padfield GD. Helicopter flight dynamics: the theory and application of flying qualities and simulation modelling. Blackwell Publishing; 2007.
[32] Tomas-Rodriguez M, Sharp R. Automated modeling of rotorcraft dynamics with special reference to autosim. In: Automation science and engineering, CASE 2007 IEEE international conference; 2007. p. 974–9.
[33] Mechanical simulation corporation, VehicleSim browser reference manual for BikeSim, CarSim, and TruckSim, Mechanical Simulation. http://www.carsim.com; 1997–2008 [accessed 31.07.17].
[34] Yeo H, Chopra I. Coupled rotor/fuselage vibration analysis using detailed 3-D airframe models. Math Comput Model 2001;33:1035–1054.
[35] Siva C, Murugan MS, Ganguli R. Effect of uncertainty on helicopter performance predictions. Proc Ins Mech Eng Part G 2009. doi:10.1243/09544100JAERO638.
[36] Castillo-Rivera S, Tomas-Rodriguez M. Helicopter flap/lag energy exchange study. Nonlinear Dyn 2017;88(4):2933-2946.
[37] Verdult V, Lovera M, Verhaegen M. Identification of linear parameter-varying state-space models with application to helicopter rotor dynamics. Int J Control 2004;77(13):1149–1159.
[38] Talebi S, Uosofvand H, Ariaei A. Vibration analysis of a rotating closed section composite Timoshenko beam by using differential transform method. J Appl Comput Mech 2015;1(4):181–86.
[39] Santos IF, Saracho CM, Smith JT, Eiland J. Contribution to experimental validation of linear and non-linear dynamic models for representing rotor-blade parametric coupled vibrations. J Sound Vib 2004;271(3-5):883–904.
[40] Ren B, Ge SS, Chen C, Fua CH, Lee TH. Modeling, control and coordination of helicopter systems. Springer; 2012.